

# ***'Breathing' of the lead–acid battery negative plate during cycling***

D. PAVLOV, S. IGNATOVA

*Central Laboratory of Electrochemical Power Sources, Bulgarian Academy of Sciences, Sofia 1040, Bulgaria*

Received 20 August 1986; revised 23 September 1986

By measuring the thickness of the negative plates with and without an expander, during cycling, it was established that the active mass volume pulsates, expanding during discharge and shrinking during charge. This phenomenon is due to the mechanical stress in the lead skeleton structure caused by the  $\text{PbSO}_4$  crystals. At each pulsation of the plate, slight changes in the structural parameters of the active mass are observed. These changes accumulate during cycling causing expansion or shrinking of the active mass. As a result of this the capacity of the plate decreases. These changes in the plate structure depend strongly on the expander.

## **1. Introduction**

During lead–acid battery operation the active mass of the negative plate often expands considerably and part of it sheds off. This phenomenon may determine the life span of the battery. It has been established that during battery cycling the expander is adsorbed on the lead surface [1–7], which affects the rates of nucleation and crystal growth, and promotes the formation of small spherical or needle-like lead crystals [8–10]. It has also been established that the expander changes both the size and morphology of the  $\text{PbSO}_4$  crystals [2, 7, 11, 12]. The phenomenon of plate expansion during cycling is connected with the changes in the organization of the active mass structure.

The negative active mass structure consists of two levels [13–15]:

(i) a skeleton built of interconnected, dendrite-like lead crystals formed during the first stage of formation; macropores are formed between the skeleton branches;

(ii) an energetic structure consisting of lead crystals grown on the skeleton during the second stage of formation. These all take part in the discharge and are again formed during the plate charge [13, 14]. During cycling with deep discharges only about 10–15% of the skeleton

structure takes part in the current generation [13].

Lead has a mole volume of  $12.28 \text{ cm}^3 \text{ mol}^{-1}$ , while that of  $\text{PbSO}_4$  is  $47.96 \text{ cm}^3 \text{ mol}^{-1}$ . A juxtaposition of these data shows that during oxidation of lead to  $\text{PbSO}_4$  the solid phase volume increases considerably. This increase is incorporated by firstly the volume of the active mass pores which decrease in cross-section and volume and secondly by the total plate volume which increases.

The purpose of this paper is to examine these phenomena during discharge and charge, as well as to establish how the expander affects the changes in the active mass dimensions.

## **2. Methods**

### *2.1. Preparation of the negative plates and test cells*

Plant-produced SLI grids, prepared from lead, 6% antimony, 0.1% arsenic and 0.1% tin alloys, were used. The active mass was prepared according to the following method. Oxidized mill lead powder was mixed in a laboratory mixer with 0.2% carbon black, 0.4%  $\text{BaSO}_4$  and 0.6% expander (sodium lignosulphatate, NaLS, or Syntan NK, SNK) and while stirring, water and

a  $\text{H}_2\text{SO}_4$  solution (specific gravity 1.4) were added, so that a paste with a 4.5%  $\text{H}_2\text{SO}_4$  to  $\text{PbO}$  ratio was prepared. The paste was stirred for 40 min at  $30^\circ\text{C}$ . The ratio between the liquid and solid phases was chosen so that the resulting paste density was  $4.2\text{ g cm}^{-3}$ . The grids were manually pasted. The plates were left to cure for 3 days at  $40^\circ\text{C}$  and 100% humidity; they were then formed in a  $\text{H}_2\text{SO}_4$  solution with a specific gravity of 1.05 and at a current density of  $4\text{ mA cm}^{-2}$  for a period of 20 h. After formation the plates were washed with water and dried in argon. They were used to make up cells with one tested negative and two plant-produced positive plates. Three types of plate were prepared: the first with negative plates without an expander, the second with NaLS expander and the third with SNK. Three cells from each type were subjected to testing. The rated capacity of the negative plates was 11 Ah at an active mass utilization of 42%.

### 2.2. Measurement of the active mass parameters during cycling and charge-discharge

The cells were subjected to automatic cycling with a charge for 9 h and a discharge for 3 h with a current of 2 A per cell. After a certain number of cycles (5, 30 etc.) cycling was interrupted and the following parameters were determined.

(i) The thickness of the negative plate in eight strictly determined spots (measured by a micrometer). The thickness of the charged plates was first determined. The cell was discharged with a current  $i = 0.25C_4\text{ A}$  (where  $C_4$  is the capacity at a 4-h discharge) up to 0 V (vs a  $\text{Hg}/\text{Hg}_2\text{SO}_4$  electrode) and the plate thickness in the same spot was again measured. The plate was then put back into the cell, left at an open circuit for 16 h and the plate thickness was measured again. After the cell was charged with a current of  $0.1C_4\text{ A}$  for 16 h the measurements of the thickness were repeated. The cells were then put onto automatic charge-discharge cycling.

(ii) Porosimetric investigations. The dependence of the pore volume distribution on the pore radius was determined by the method described in [16, 17].

(iii) Active mass structure. By means of SEM observations the active mass structure (of charged

and discharged cells) and the morphology of the  $\text{PbSO}_4$  crystals after a period of open circuit in  $\text{H}_2\text{SO}_4$  were determined. The skeleton of the active mass was examined by placing parts of the discharged active mass in a solution of 15%  $\text{NH}_4\text{CH}_3\text{COOH}$  and 5%  $\text{CH}_3\text{COOH}$  at  $100^\circ\text{C}$  for 30 min. These parts were then washed with water and dried in argon prior to observation by SEM.

## 3. Results and discussion

### 3.1. Plate pulsation during cycling

The changes in the thickness of the three types of negative plates are presented in Fig. 1. The measurements were taken after a charge, a discharge, an open circuit period and again after a charge. The results are from measurements carried out at two different, strictly determined spots of the plate. Data on the remaining six spots are similar.

Two kinds of processes are related to the changes in the plate thickness.

(i) Quasi-reversible. These proceed within one cycle and cause pulsation of the plate. There exists a general rule: during discharge the plate thickness increases, while during the open circuit pause of the discharged plate its thickness decreases slightly, and during charge it shrinks towards its initial value.

(ii) Irreversible. These occur over a long period of time (e.g. 50–70 cycles). The restoration of the initial plate thickness after charge seldom occurs. This indicates that during pulsation some changes occur in the active mass structure. With cycling these changes are accumulated, as a result of which the plate may expand or shrink. Thus Fig. 1 shows that when the plates do not contain an expander the tendency towards shrinking is very pronounced. In the plates containing the expander NaLS, the thickness first increases (30 cycles) and then tends to its initial value (60–70 cycles), the intensity of pulsation being of the same order as that in the initial cycles. In the plates with SNK both the thickness of the plate and the intensity of the pulsation decrease slowly. A comparison of Figs 1b and 1c shows that the influence of the NaLS expander remains the same even after the 72nd

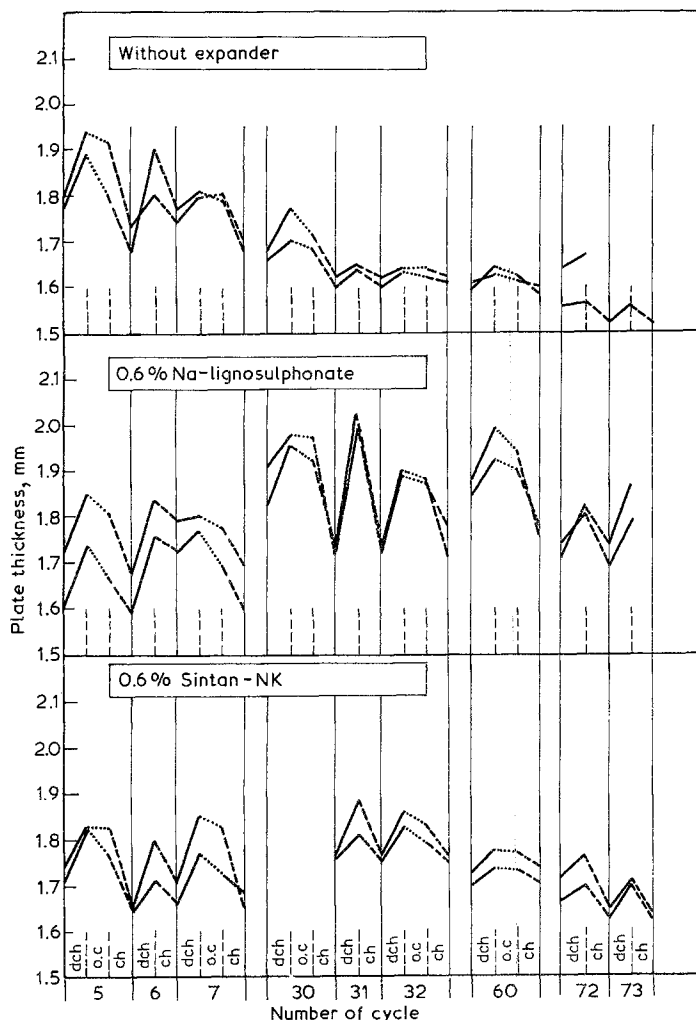


Fig. 1. Changes of the thickness of the plate with active mass without an expander and with NaLS or SNK expanders. The measurements carried out in two spots of the plate are presented. — (dch) discharge; ··· (o.c.) open circuit; --- (ch) charge.

cycle, while that of the SNK decreases; this may imply that the latter is chemically more unstable and disintegrates during cycling.

3.2. The ability of the pore volume to incorporate the increase of the solid phase during discharge

The total volume of the pores,  $V_{por}$ , was experi-

mentally determined by means of mercury porosimetry. In order to avoid amalgam formation, the lead surface had been previously covered with stearic acid. On the basis of Faraday's law the increase of the solid phase volume during discharge ( $V_r = V_{PbSO_4} - V_{Pb}$ ) was calculated. These data are presented in Table 1.

The table shows that the volume of the pores is quite sufficient to incorporate the whole

Table 1.

	$V_{por}$ ( $cm^3 g^{-1}$ )	$V_r$ ( $cm^3 g^{-1}$ )	$\Delta V = V_{por} - V_r$ ( $cm^3 g^{-1}$ )	$\frac{\Delta V}{V_{por}}$ (%)
Without an expander	0.1138	0.0740	0.0398	35%
0.6% NaLS	0.1346	0.0879	0.0467	35%
0.6% SNK	0.1208	0.0890	0.0318	26%

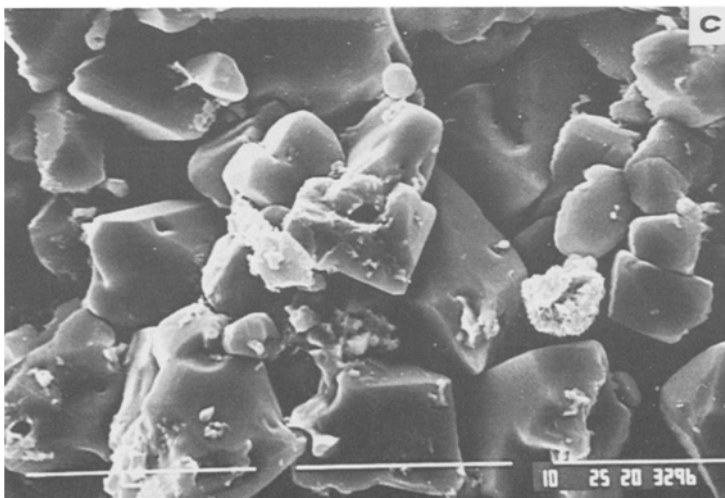
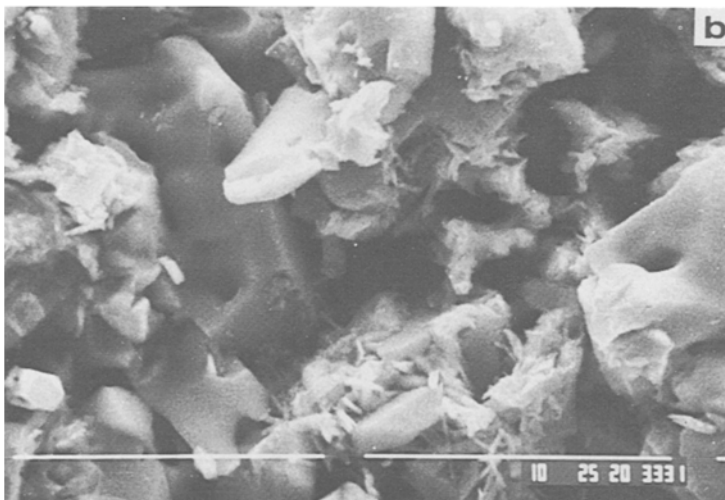
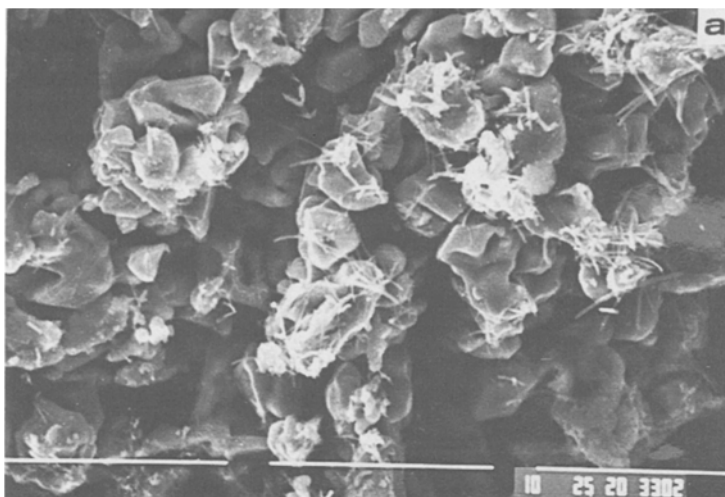


Fig. 2. SEM micrographs of the active mass: (a) charged, (b) discharged, (c) discharged, and kept in a  $H_2SO_4$  solution for 16 h. The plate is without an expander during the seven cycles. Scale bar:  $10\ \mu m$ .

increase of the solid phase volume caused by the formation of  $PbSO_4$ . After the charge, one quarter to one third of the pore volume remains free. Hence, the active mass pulsation at discharge and charge is due to the nature of the processes of  $PbSO_4$  crystallization which cause stress and expansion of the active mass.

### 3.3. Processes causing the plate pulsation

Fig. 2 shows the SEM micrographs of the active mass without expander at the 7th cycle. Fig. 2a shows the energetic structure of a charged active mass, consisting of strongly folded dendrites. A micrograph of a discharged active mass is shown

in Fig. 2b. During the discharge, lead dendrites are oxidized to  $PbSO_4$  crystals. The latter are intimately incorporated into the skeleton structure. The crystal nucleation and growth proceed probably under strong oversaturation and that is why the  $PbSO_4$  crystals have an irregular shape. Since the resulting product of the reaction ( $PbSO_4$ ) has a greater volume than the initial product (lead) the active mass is subjected to mechanical stress and expansion during the formation of  $PbSO_4$ . The plate increases in thickness (Fig. 1).

It is obvious that the initially formed  $PbSO_4$  crystals are not in equilibrium. At idle time recrystallization occurs. Most probably some of

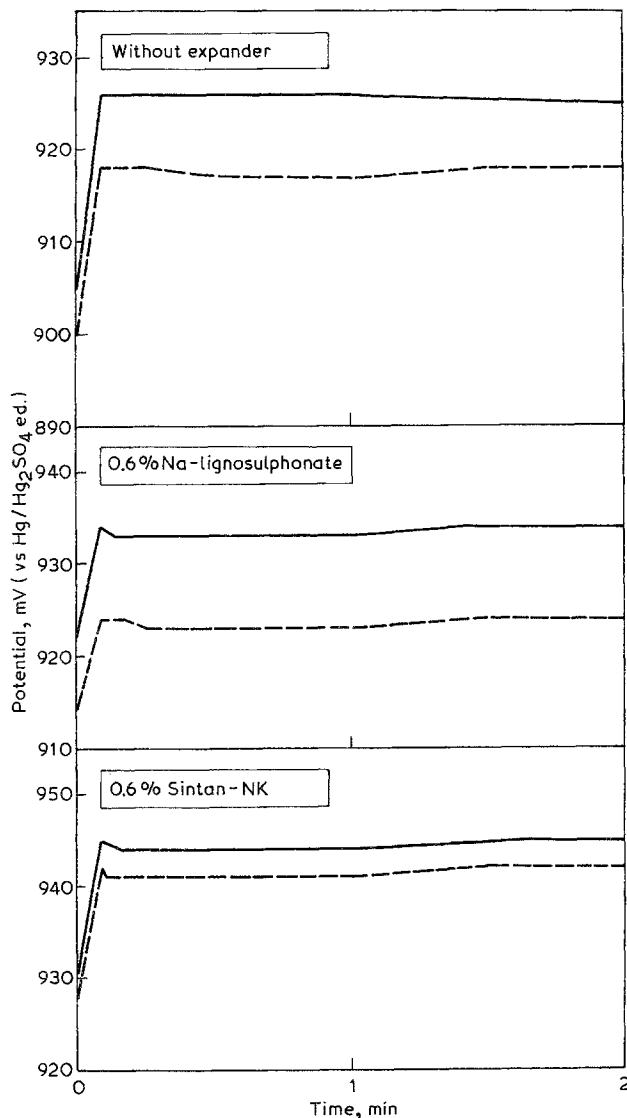


Fig. 3. Changes of the potential of the plates during charge at the 30th and 31st cycles. — Charge after open circuit; --- charge after discharge.

the  $\text{PbSO}_4$  crystals dissolve and other crystals grow, tending to form well-shaped faces (Fig. 2c). During this process the mechanical stress within the active mass partially decreases and the plate shrinks slightly. At charge the  $\text{PbSO}_4$  crystals dissolve and  $\text{Pb}^{2+}$  ions are reduced to lead energetic crystals. The plate shrinks, tending to resume its initial thickness (Fig. 1). Hence, the discharge process proceeds in two stages, the first being the oxidation of lead to non-equilibrium  $\text{PbSO}_4$  crystals and the second being the recrystallization of these non-equilibrium  $\text{PbSO}_4$  crystals.

### 3.4. *Effect of the $\text{PbSO}_4$ crystal type on the charge process*

It may be expected that the above two types of  $\text{PbSO}_4$  crystals will affect the charge process. Fig. 3 shows the potential transients of plates which were charged immediately after discharge as well as such charged after an open circuit period. The charge current was 2 A per cell.

The potential of the plate charged after a period of open circuit is slightly higher than that of the plate charged immediately after discharge. The dissolution rate of the equilibrium  $\text{PbSO}_4$

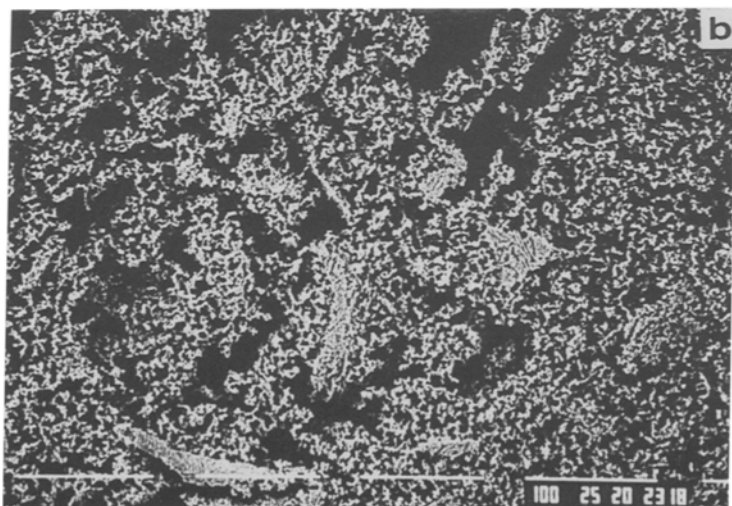
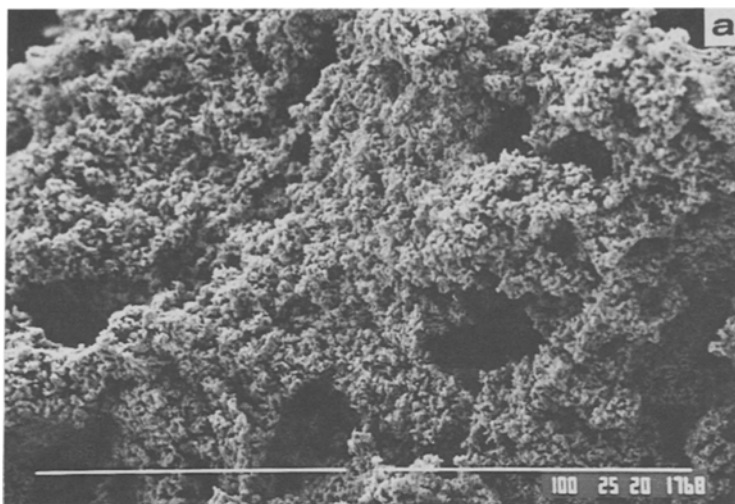


Fig. 4. Macrostructure of (a) the charged active mass, (b) the skeleton at the 32nd cycle. Scale bar: 100  $\mu\text{m}$ .

crystals is probably smaller than that of the non-equilibrium ones. Besides, after recrystallization the structure of the active mass eventually poses greater transport hindrances to the movement of the ion flows.

### 3.5. Changes in the skeleton structure during cycling

The skeleton is the mechanical carrier of the energetic structure and the conductor of the electrons to every point of the active mass. The active mass of a charged plate is shown in Fig. 4a, while the skeleton of the above plate after discharge is shown in Fig. 4b. The plate is without an expander and has undergone 32 cycles.

During cycling the structure of the active mass loses its macrohomogeneity. There could be two factors causing this.

(i) 'Breathing' of the active mass. During discharge the formation and growth of  $\text{PbSO}_4$  crystals occurs most intensively at those sites of the cross-section of the plate where the macropores allow the easiest exchange of ionic flows with the bulk of the electrolyte. This leads to a concentration of the mechanical stress within these zones as a result of which the skeleton breaks in some places. It can be presumed that a certain number of these cleavages in the skeleton during charging will be repaired, but new ones will appear during discharge. It is probable that a certain concentration of cracks, caused by the active mass pulsation, is maintained during cycling.

(ii) Formation of hydrogen bubbles inside the active mass. When hydrogen is evolved the bubbles formed start growing. In certain places they cleave the skeleton, forming large furrows and caves. In other places the skeleton may shrink and the micropores are plugged. Hence, the formation of caves and furrows in the active mass is a second factor causing irreversible changes in the active mass structure. This depends on the distribution of antimony or of the other additives decreasing the hydrogen overvoltage. These additives deposit during battery operation.

These irreversible processes cause changes in the flows within the active mass. During

cycling, if the discharge rate in some regions of the active mass is higher, the skeleton there can take a more active part in the discharge reaction, as a result of which its branches can become thinner. This leads to an increase of the inner ohmic resistance of the skeleton at that place, and the reaction rate decreases. These processes lead to an inner self-regulation of the rate of the processes in the volume of the active mass.

### 3.6. Changes in the skeleton as a result of the irreversible processes

Fig. 5 presents the micrograph of the skeleton at the 7th and the 60th cycle.

*3.6.1. Active mass without an expander.* Fig. 5a and 5b show that, during cycling, the thickness of the skeleton dendrites has increased and the pore volume between them has decreased. This leads to the formation of a sound and stable skeleton capable of enduring the mechanical stress, as a result of which the plate pulsation is small. Indeed, Fig. 1a shows that after the 60th cycle the changes in the thickness of the plate during a single cycle are negligible.

*3.6.2. Active mass with NaLS expander.* Fig. 5c and 5d show that, during cycling, the thickness of the skeleton branches has not changed and they have remained thin. The active mass has expanded as a consequence of the formation of caves and furrows caused by the released hydrogen and the active mass pulsation. As a result of this the skeleton has become less stable. Such a skeleton is not able to withstand the mechanical stress appearing during the discharge and the 'breathing' is 'deep'. This is shown in Fig. 1b.

*3.6.3. Active mass with a SNK expander.* Fig. 5e and 5f show that after 60 cycles a large part of the skeleton branches have become thick. In spite of the great number of caves in the skeleton branches, such a structure is on the whole stable and can withstand the mechanical stress appearing during cycling. Fig. 1c shows that after the 60th cycle the 'breathing' of these plates is 'on the surface'.

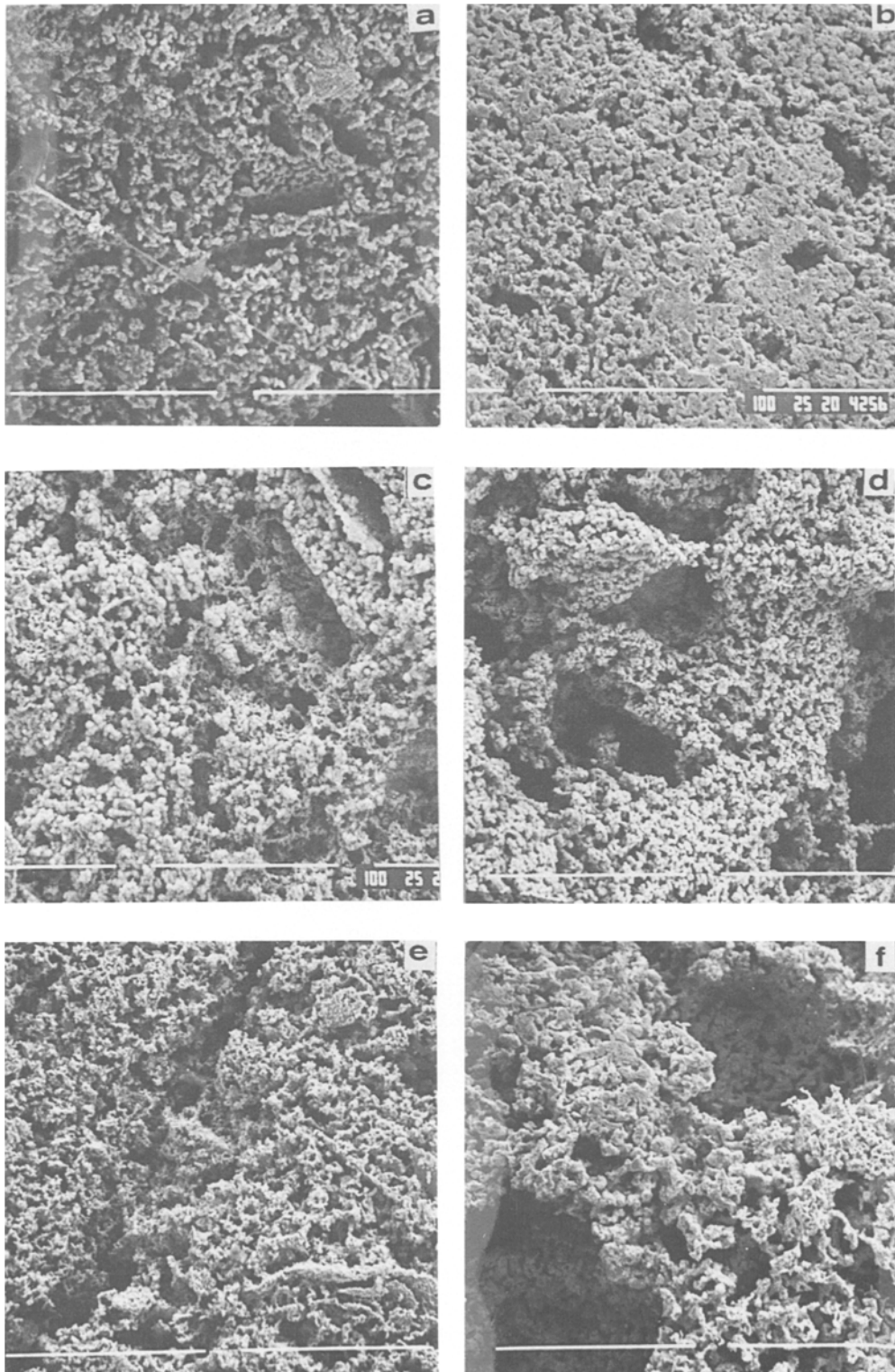


Fig. 5. SEM micrographs of the skeleton of the active mass at the 7th cycle (a, c, e) and the 60th cycle (b, d, f) of plates without an expander (a, b), with NaLS (c, d) and with SNK (e, f). Scale bar: 100  $\mu\text{m}$ .



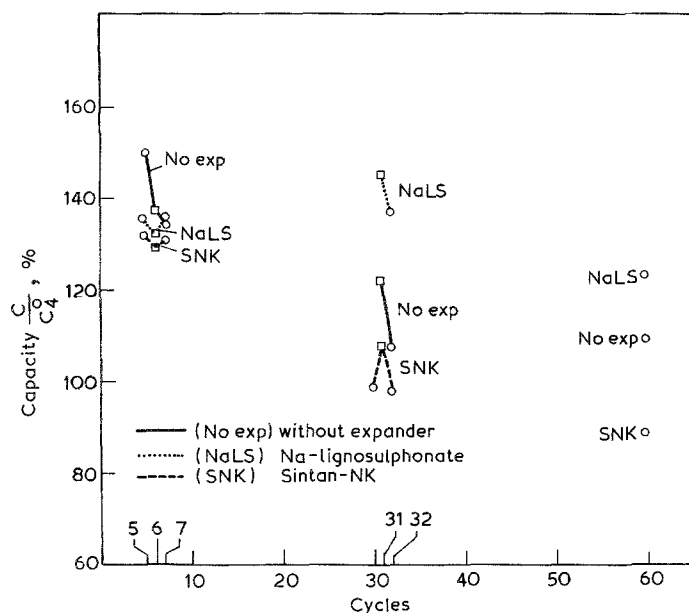


Fig. 6. Influence of the number of cycles on the capacity for the three types of cells. The preceding cycle contains: □, discharge and open circuit periods; ○, discharge period.

### 3.7. Influence of the skeleton structure changes on the plate capacity

The experimentally determined capacity values in percentage versus the rated capacity during cycling are presented in Fig. 6. It can be seen that the capacity of the plates without an expander and with an SNK expander decrease with cycling. At the same time, the difference between the values of the capacity at the 6th and the 60th cycles of the plates with NaLS are very small. If the results are compared with the curves in Fig. 1 it can be seen that there is not a direct connection between the values of the capacity and the 'breathing' of the active mass. However, on comparing Figs 1, 5 and 6 it can be seen that as a result of the 'breathing' the initially created (during formation) organization of the active mass structure gradually disintegrates and the stability of the skeleton structure changes. This affects the plate capacity.

### Acknowledgement

The authors acknowledge the technical assistance of Mrs Stambolska.

### References

- [1] T. Sharpe, *Electrochim. Acta* **1** (1969) 635.
- [2] J. R. Pierson, P. Gurlusky, A. C. Simon and S. M. Caulder, *J. Electrochem. Soc.* **117** (1970) 1463.
- [3] M. P. J. Brennan and N. A. Hampson, *J. Electroanal. Chem.* **48** (1973) 465.
- [4] E. G. Yampol'skaya and B. N. Kabanov, *Sov. J. Appl. Chem.* **37** (1964) 2530.
- [5] G. Archdale and J. A. Harrison, *J. Electroanal. Chem.* **47** (1973) 93.
- [6] A. Le Mehaute, *J. Appl. Electrochem.* **6** (1976) 543.
- [7] B. K. Mahato, *J. Electrochem. Soc.* **127** (1980) 1679.
- [8] A. C. Simon, S. M. Caulder, P. J. Gurlusky and J. R. Pierson, *Electrochim. Acta* **19** (1974) 739.
- [9] *Idem*, *J. Electrochem. Soc.* **121** (1974) 463.
- [10] A. C. Simon, C. P. Wales and S. M. Caulder, *ibid.* **128** (1981) 236.
- [11] E. G. Yampol'skaya, M. I. Ershova, I. I. Astahov and B. N. Kabanov, *Electrochim. Acta* **2** (1966) 1327.
- [12] E. G. Yampol'skaya, M. I. Ershova, V. V. Surinov, I. I. Astahov and B. N. Kabanov, *Electrochim. Acta* **8** (1972) 1209.
- [13] D. Pavlov and V. Iliev, *J. Power Sources* **7** (1981) 153.
- [14] V. Iliev and D. Pavlov, *J. Appl. Electrochem.* **15** (1985) 39.
- [15] D. Pavlov, E. Bashtavelova and V. Iliev, in 'Advances in Lead-Acid Batteries' (edited by K. R. Bullock and D. Pavlov), Proceedings Vol. 84-14, 166 Meeting of ECS, New Orleans (1984) p. 16.
- [16] M. Svata, 'Porosimetrie a její pouziti', Czech. Acad. Sci., Praha (1969) p. 94.
- [17] D. Pavlov, V. Iliev, G. Papazov and E. Bashtavelova, *J. Electrochem. Soc.* **121** (1974) 854.